The Journal of Chemical Physics

Design and application of a multicoefficient correlation method for dispersion interactions

Cite as: J. Chem. Phys. **120**, 590 (2004); https://doi.org/10.1063/1.1630955
Submitted: 19 May 2003 . Accepted: 14 October 2003 . Published Online: 31 December 2003

Timothy J. Giese, and Darrin M. York

Design and application of a multicoefficient correlation method for dispersion interactions

Timothy J. Giese and Darrin M. York[a)]
Department of Chemistry, University of Minnesota, Minneapolis, Minnesota 55415

(Received 19 May 2003; accepted 14 October 2003)

A new multicoefficient correlation method (MCCM) is presented for the determination of accurate van der Waals interactions. The method utilizes a novel parametrization strategy that simultaneously fits to very high-level binding, Hartree–Fock and correlation energies of homo- and heteronuclear rare gas dimers of He, Ne, and Ar. The decomposition of the energy into Hartree–Fock and correlation components leads to a more transferable model. The method is applied to the krypton dimer system, rare gas–water interactions, and three-body interactions of rare gas trimers He_3, Ne_3, and Ar_3. For the latter, a very high-level method that corrects the rare-gas two-body interactions to the total binding energy is introduced. A comparison with high-level CCSD(T) calculations using large basis sets demonstrates the MCCM method is transferable to a variety of systems not considered in the parametrization. The method allows dispersion interactions of larger systems to be studied reliably at a fraction of the computational cost, and offers a new tool for applications to rare-gas clusters, and the development of dispersion parameters for molecular simulation force fields and new semiempirical quantum models. © *2004 American Institute of Physics.*
[DOI: 10.1063/1.1630955]

I. INTRODUCTION

The study of weak dispersion forces, or van der Waals (vdW) forces, has been and continues to be of great interest in theoretical chemical physics.[1–3] Rare gases have served as the benchmark system to study these weak interactions with both experimental[4,5] and theoretical methods.[1–3] To calculate accurate potential energy surfaces for rare-gas interactions presents special challenges. The binding energy of these systems arises almost entirely from electron correlation (beyond Hartree–Fock), and hence requires high-level *ab initio* methods for an accurate treatment.[6–14] Density-functional methods have traditionally been unsatisfactory in describing dispersion interactions,[15] although some progress has been made,[16–20] and this remains an important area of research.

The very weak binding energies of vdW systems necessitates special consideration with respect to basis set size and superposition error. Extensive theoretical investigations have found that sufficiently high levels of theory,[21–28] combined with large basis sets[21,27–37] with bond functions,[21,27,38–43] and counterpoise correction[21,27,28] are sufficient to accurately characterize the dimer interactions. At this time, such rigor is prohibitively time consuming (and less straightforward) to apply to larger vdW clusters in a practical way. Nonetheless, the study of rare-gas clusters with theoretical methods is of great interest not only for chemical physics, but also to obtain a detailed understanding of the many-body nature of dispersive interactions and serve as a benchmark for the development of transferable many-body force fields or semiempirical quantum models. Consequently, the development of a more tractable electronic structure method is a necessary first step toward the study of vdW clusters using supermolecular approaches.

The goal of the present work is to develop a method that is able to reproduce highly accurate dimer potential (binding energy) curves[44–46] in a tractable manner (preferably *without* counterpoise corrections) that can be extended to larger clusters. Specifically, the potential energy curves for He–He, Ne–Ne, Ar–Ar, He–Ne, He–Ar, and Ne–Ar are considered. Potential energy surfaces of He–He, Ne–Ne, Ar–Ar, Kr–Kr, Xe–Xe,[45] and all possible sets of heteronuclear dimers[46] have been fit to spectroscopic data. The resulting potential surfaces are valid near the potential energy minimum but not valid at large and small internuclear distances. Cybulski and co-workers[21] calculated the counterpoise corrected potential energy of He–He, Ne–Ne, Ar–Ar, He–Ne, He–Ar, and Ne–Ar with CCSD(T)/aug-cc-pV5Z supplemented with a set of $(3s3p2d2f1g)$ bond functions at 13 different internuclear separations in the range of *roughly* 2–7 Å for each dimer. Recently, the protocol of Cybulski and co-workers[21] has been applied to these systems and extended to include 100 points for each dimer curve over a larger range and analyzed in greater detail with respect to the correlation energy and second virial coefficients.[44]

In this work, a multicoefficient correlation method (MCCM) for the calculation of the dimer interaction energies is presented. A MCCM is a linear combination of energies corresponding to various levels of theory and basis sets parametrized to reproduce the energy one would obtain at a very high level of theory and very large basis set. The MCCM presented here is analogous to those of Fast and Truhlar[47] and inspired by the original work of Pople and co-workers.[48,49] The parametrization of the MCCM method is based on the recently reported high-level potential energy

a)Corresponding author. Electronic mail: york@chem.umn.edu

curves.[44] The MCCM method developed here introduces several novel features (see below) that differentiate it from other MCCM models, and for the purpose for which it was designed, offers some considerable advantages.

The outline of the paper is as follows: In Sec. II we establish the relevant background. In Sec. III we describes the methods, including a brief summary of the calculation of the dimer reference potentials, the form of the MCCM, and the parametrization techniques employed. In Sec. IV we present the fitted MCCM coefficients and compare the MCCM interaction potential to the reference potential, to other theoretical work, and to the experimentally derived potentials of Ogilvie and Wang,[45,46] who reparametrized the piecewise continuous experimental potentials of Aziz and collaborators.[50–58] In Sec. V we conclude the paper with a summary of results and discussion of future research directions.

II. BACKGROUND

The goal of this work is to design a computationally tractable quantum method to accurately calculate the potential energy surfaces of vdW clusters. These surfaces can be used as benchmarks to characterize many-body effects for systems that are largely devoid of electronic polarization, and hence allow focus to be placed on the exchange and correlation contributions. The nature of many-body exchange and correlation are fundamental features that will play an important role in the development of new-generation molecular simulation force fields[59–61] and semiempirical quantum models.

The weak binding of rare gas dimers arises from van der Waals dispersion interactions that are inherently an electron correlation effect. This has the consequence that calculations require a high-level treatment of electron correlation and are extremely sensitive to basis sets. It has been shown previously[21,44] that accurate, converged *ab initio* results for rare gas dimers can be obtained at the CCSD(T) level with very large basis sets. These calculations required the use of a singly augmented basis (aug-cc-pV5Z) with additional bond functions[39,42] and counterpoise corrections to avoid problems associated with basis set superposition error (BSSE).[62,63] The computational requirement of these high-level calculations preclude their application to even an argon trimer or krypton dimer system without very extensive resources. These results inspired work to develop a method that could overcome the present bottlenecks.

The approach taken here was to adopt a multicoefficient correlation method for dispersion interactions that does not require *simultaneously* the use of large basis sets and highly correlated levels of theory. Moreover, the method does not employ bond functions or counterpoise corrections, both of which become tedious to apply to clusters. For clusters, both bond functions and counterpoise corrections have disadvantages.[42,64] The use of multilevel methods has gained much success in the recent literature for the calculation of thermochemical data[47–49,65–81] and molecular geometry.[65,80–82] To date, no MCCM has been reported that has been designed for systems bound primarily by dispersion interactions. One of the main premises of the multicoefficient methods is that one can extrapolate to the high theoretical level/large basis set limit by taking advantage of the additivity of these effects. Models can be constructed that are linear combinations of theoretical levels and basis sets that, when combined, yield highly accurate results, but that never require a highly correlated theoretical calculation to be performed with a large basis set. The result is that high accuracy can often be obtained for a fraction of the computational effort required by a single sufficiently high theoretical level and basis set.

III. METHODS

A. The MCCM model

The theoretical levels employed to develop the MCCM model included Hartree–Fock (HF), Möller–Plesset second-order perturbation (MP2), coupled-cluster singles and doubles (CCSD) and perturbative triples [CCSD(T)]. These theoretical levels have a systematic hierarchy in that, for most electronic structure packages, a calculation at any of these levels requires calculations at all of the lower levels to precede, and so these energies are typically available at no extra computational cost. The basis sets used in the model were the singly augmented correlation-consistent basis sets of Dunning[29] (aug-cc-pVDZ, aug-cc-pVTZ, aug-cc-pVQZ, aug-cc-pV5Z). The shorthand notation ''aDZ,'' ''aTZ,'' ''aQZ,'' and ''a5Z'' for these basis sets is introduced and used in subsequent equations and discussion.

In order to differentiate the model presented here from existing models, the acronym MCCM–vdW (Multi-Coefficient Correlation Method–van der Waals) is used. MCCM–vdW has ten parameters (nine independent degrees of freedom; see below) and requires calculations at the CCSD(T)/aDZ, CCSD/aTZ, MP2/aQZ, and HF/a5Z levels.

The expression for the MCCM–vdW energy is given by

$$E(\mathrm{MCCM-vdW}) = a_1 E(\mathrm{HF/aDZ}) + a_2 E(\mathrm{MP2/aDZ}) + a_3 E(\mathrm{CCSD/aDZ}) + a_4 E(\mathrm{CCSD(T)/aDZ}) + a_5 E(\mathrm{HF/aTZ}) + a_6 E(\mathrm{MP2/aTZ}) + a_7 E(\mathrm{CCSD/aTZ}) + a_8 E(\mathrm{HF/aQZ}) + a_9 E(\mathrm{MP2/aQZ}) + a_{10} E(\mathrm{HF/a5Z}), \quad (1)$$

where the a_i's are a set of *linearly dependent* parameters, coupled by the constraint that the coefficients sum to unity. This particular constraint ensures that certain energy scaling relations are obeyed; for example, that one-electron systems are treated exactly (within the basis set limits), and that Coulomb interactions have the proper long range behavior. Not all MCCM-type models obey this constraint condition.

The total energy can be decomposed into a Hartree–Fock self-consistent field (HF-SCF) energy term, E_{HF}, and a correlation energy term, E_C:

$$E = E_{\mathrm{HF}} + E_C . \tag{2}$$

The MCCM–vdW model for the correlation energy is given by

$$\begin{aligned} E_C(\mathrm{MCCM\text{–}vdW}) = {} & a_2(E(\mathrm{MP2/aDZ}) - E(\mathrm{HF/aDZ})) + a_3(E(\mathrm{CCSD/aDZ}) - E(\mathrm{HF/aDZ})) + a_4(E(\mathrm{CCSD(T)/aDZ}) \\ & - E(\mathrm{HF/aDZ})) + a_6(E(\mathrm{MP2/aTZ}) - E(\mathrm{HF/aTZ})) + a_7(E(\mathrm{CCSD/aTZ}) - E(\mathrm{HF/aTZ})) \\ & + a_9(E(\mathrm{MP2/aQZ}) - E(\mathrm{HF/aQZ})). \end{aligned} \tag{3}$$

The MCCM–vdW model for the HF-SCF energy is

$$\begin{aligned} E_{\mathrm{HF}}(\mathrm{MCCM\text{–}vdW}) = {} & E(\mathrm{MCCM\text{–}vdW}) - E_C(\mathrm{MCCM\text{–}vdW}) \\ = {} & (a_1 + a_2 + a_3 + a_4)E(\mathrm{HF/aDZ}) + (a_5 + a_6 + a_7)E(\mathrm{HF/aTZ}) + (a_8 + a_9)E(\mathrm{HF/aQZ}) \\ & + a_{10}E(\mathrm{HF/a5Z}). \end{aligned} \tag{4}$$

MCCM–vdW is the first MCCM method to explicitly decompose the energy into HF-SCF and correlation components. As described in great detail within Sec. III C, the parametrization of the coefficients a_{1-10} involve the simultaneous fitting of $E(\mathrm{MCCM\text{–}vdW})$, $E_C(\mathrm{MCCM\text{–}vdW})$, and $E_{\mathrm{HF}}(\mathrm{MCCM\text{–}vdW})$ to reference potential energy surfaces. The energy decomposition strategy employed here results in a MCCM–vdW model that is transferable and provides the accurate determination of the individual HF-SCF and correlation contributions to the total energy. Note that the MCCM–vdW model does not require the calculation of counterpoise corrections or the use of bond functions (although, as discussed below, it is parametrized to reference potentials that do).

B. Generating vdW dimer reference potentials

The reference dimer binding energies[44] were calculated at the CCSD(T)/a5Z level with an auxiliary set of $(3s3p2d2f1g)$ bond functions[21] located at the center of mass of the system. The binding energy of the dimer was calculated using the counterpoise method of Boys and Bernardi.[62] This protocol has been demonstrated to be highly accurate for rare-gas dimers.[21,83] The high-level reference HF-SCF energy is calculated in an analogous way as the reference binding energy, but using the the HF energies instead of the CCSD(T) values. The reference correlation energy is generated by subtraction of the reference HF-SCF energy from the reference CCSD(T) energy. All calculations were performed using MOLPRO 2000.[84]

The reference binding, HF-SCF, and correlation potential energy curves were evaluated at 100 radial points, generated from the empirical equation

$$\begin{aligned} & r_{\alpha i} = R_{\mathrm{eq}}(\alpha) \cdot (1 + \mathrm{sgn}(\Delta_\alpha + i - 1) \cdot \gamma \cdot (\Delta_\alpha + i - 1)^2), \\ & i = -\Delta_\alpha \cdots 99 - \Delta_\alpha , \end{aligned} \tag{5}$$

where "α" is an index that indicates the type dimer (see below), $R_{\mathrm{eq}}(\alpha)$ is the radial distance of the minimum on the high-level reference binding potential energy curve for the "α" dimer, $r_{\alpha i}$ is the ith radial sample point, Δ_α is an integer shift function given by $\Delta_\alpha = -\mathrm{INT}(60/\sqrt{R_{\mathrm{eq}}(\alpha)})$, and γ is a unitless parameter ($\gamma = 0.000\,36$ for all the curves in the present work). The radial sample points are thus generated from a square mesh that originates at the reference binding potential energy minimum and radiates in both directions so that there is a higher density of points clustered around the minimum. Calculated force constants and their related vibrational frequencies were determined from fitting a quadratic function to the points within 0.05 Å of the minimum using singular value decompositions. The corresponding reference values were determined, as in other work,[18] from differentiation of the analytic form of Ogilvie and Wang.[45,46]

C. The MCCM parametrization procedure

The parameters in MCCM–vdW are the coefficients a_i [Eq. (1)]. These are linear parameters in the model, and can be fit using a constrained linear least-squares method (see the Appendix). Simple scaling arguments require that the coefficients sum to unity. A singular value decomposition scheme was used to ensure the elimination of linear dependencies in the parameters. The main feature of the merit function is the inclusion of weights ω_v, ω_x, and ω_c that penalize deviations in the binding energy, HF-SCF, and correlation components of the energy differently.

IV. RESULTS AND DISCUSSION

In this section, the results of the fitting procedure are presented, the stability of the coefficients are discussed, and tests of the transferability of the coefficients are described. The outline of this section is as follows: In Sec. IV A addresses the stability of the coefficients with respect to the linear combination of potentials within the fitting function and with respect to the amount of reference data used in the fitting procedure. In Sec. IV B we compare the rare-gas dimer properties between experimentally derived potentials and those calculated by MCCM–vdW and the reference data to which it was fit. In Sec. IV C we apply MCCM–vdW to a system *not* contained in the reference data (Kr–Kr) in order to address the transferability of the coefficients. In Sec. IV D we further the discussion of transferability by applying MCCM–vdW to Rg$\cdots$H$_2$O (Rg=He, Ne, Ar) systems. Finally, in Sec. IV E, rare-gas trimers are investigated to display the usefulness of MCCM–vdW in determining three-body potential energy surfaces.

TABLE I. Stability of parameters for the MCCM–vdW model fit to different training sets.[a]

Param	Level/basis	Training set HOMO	HETERO	ALL
a_1	HF/aDZ	0.004 011 60	0.042 029 74	0.041 335 78
a_2	MP2/aDz	−0.097 933 96	−0.754 550 17	−0.403 657 30
a_3	CCSD/aDZ	1.606 533 55	1.510 648 52	1.181 703 88
a_4	CCSD(T)/aDZ	−1.724 383 23	−0.997 348 97	−1.019 065 35
a_5	HF/aTZ	−0.059 898 60	0.094 613 39	−0.044 527 48
a_6	MP2/aTZ	−0.809 315 30	−0.396 277 35	−0.699 054 45
a_7	CCSD/aTZ	1.292 396 18	0.499 299 53	0.911 509 29
a_8	HF/aQZ	−0.195 276 49	−0.649 356 31	−0.368 662 21
a_9	MP2/aQZ	0.970 589 91	1.276 184 45	1.179 344 05
a_{10}	HF/a5Z	0.013 276 34	0.374 757 16	0.221 073 78
RMSD		*0.936 658*	*0.797 115*	*0.734 623*

[a]A comparison of the stability of the unitless parameters a_k $k=1,...,10$ resulting from the constrained fitting procedure described in the text using different training sets: homodimers (HOMO), heterodimers (HETERO) or both (ALL). In all cases, the weights in Eq. (24) were set to $\omega_v=0.8$, and $\omega_x=\omega_c=0.1$. The parameters fit to ALL correspond to the MCCM–vdW model presented here and are shown in boldface type.

A. Fitting the MCCM–vdW coefficients

In this section, a comparison of results obtained from different fitting schemes (see the Appendix) is provided, as well as an analysis of the stability of the fitting coefficients in the MCCM–vdW model.

A detailed discussion of the fitting errors with respect to choice of weights $(\omega_v,\omega_x,\omega_c)$ and training set (homonuclear, heteronuclear, and all dimers) is presented in the EPAPS supplementary material to the document.[85] Upon inspection, the weight scheme (see the Appendix) $\omega_v=0.8$, $\omega_x=0.1$, $\omega_c=0.1$ was chosen.

The comparison of the MCCM–vdW fitting coefficients using this weight scheme but obtained with the different training sets are compared in Table I. The coefficients are not widely oscillating, but also are not identical. The fit to *ALL* has the lowest coefficient root mean square deviation, and was observed to be overall the most stable and transferable.

The overall transferability of the model with respect to training sets is quite good (see EPAPS supplementary material[85]), despite significant differences in the coefficients given in Table I. The MCCM–vdW parameters shown in boldface in Table I correspond to constrained minimization of $\chi^2(\mathbf{a};0.8,0.1,0.1,ALL)$, and are the parameters that for the MCCM–vdW model applied and discussed in the remainder of the paper.

In summary, fitting to the HF-SCF, correlation, and total interaction potentials stabilize the coefficients relative to fitting the total binding potential energy alone. This is suggestive that consideration of individual HF-SCF and correlation components may result in more transferable quantum models. The parameters were observed to be insensitive to nonzero values of ω_x and ω_c.

B. Validation of the MCCM–vdW model

Figure 1 compares the MCCM–vdW and high-level reference potential energy curves (SCF, correlation, and overall interaction). The MCCM–vdW potentials fit the reference potentials *relatively* well. The most noticeable deviation in the fit is He–He, which is caused by the difficulty in fitting the relatively very weak correlation potential. He–He proves difficult to fit in relation to the other potential surfaces due to the very small binding and correlation energies. The He–He van der Waals potential is notoriously difficult, and has been the topic of numerous investigations.[26,50,86–95] The fitting procedure weights each potential curve equally with respect to the dimer; i.e., the He–He potential energy curves are weighted in the same manner as the Ar–Ar potential energy curves. In fact, in an absolute sense, the error in the MCCM–vdW potentials for He–He is fairly small; however, the relative error is significantly larger. The fitting procedure could be modified so as to use the relative weights for each curve, and, in fact, that was one of the many schemes that was tested. The He–He curves present special challenges, and increasing the weight in order to fit the curve simultaneously with the other curves lead to a less overall reliable model.

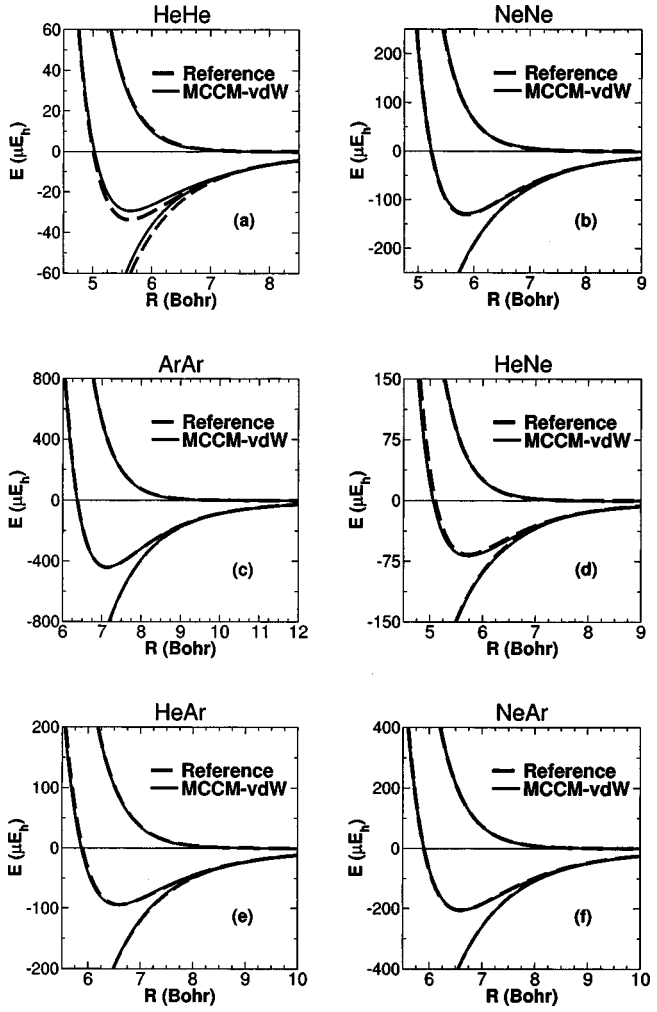

FIG. 1. A comparison of the fitted MCCM–vdW potentials with the reference potentials. For clarity, the MCCM–vdW potential is defined by the χ^2 merit function $\omega_v=0.8$, $\omega_x=0.1$, $\omega_c=0.1$ upon fitting to the hetero- and homodimers of He, Ne, and Ar.

The equilibrium distance (R_e), well depth (D_e), frequency (ω_e), and force constant (k_e) are listed for the homodimer potential energy curves and heterodimer curves (Table II). In general, the fitted MCCM–vdW model repro-

TABLE II. A comparison of MCCM–vdW with the high-level reference and experimentally derived potential energy curves for rare-gas dimers.[a]

		a.u.	μE_h		μa.u.	
Dimer	Source	$\mathbf{R_e}$	$\mathbf{D_e}$	$\mathbf{D_0}$	$\boldsymbol{\omega_e}$	$\mathbf{k_e}$
	MCCM–vdW	5.641	29.30	⋯	133.30	65.30
He–He	Reference	**5.626**	**33.68**	⋯	**149.20**	**81.81**
	OW	*5.612*	*34.74*	⋯	*150.72*	*83.47*
	MCCM-vdW	5.874	128.13	73.77	127.66	301.91
Ne–Ne	Reference	**5.857**	**130.44**	**74.14**	**132.36**	**324.58**
	OW	*5.841*	*133.80*	*77.22*	*129.49*	*310.65*
	MCCM–vdW	7.137	440.74	374.50	148.49	808.69
Ar–Ar	Reference	**7.141**	**441.83**	**375.33**	**137.85**	**696.97**
	OW	*7.099*	*453.56*	*386.11*	*140.51*	*724.05*
	MCCM–vdW	5.724	68.34	13.37	158.08	153.25
He–Ne	Reference	**5.725**	**66.59**	**11.75**	**162.68**	**162.30**
	OW	*5.728*	*65.54*	*11.42*	*158.72*	*154.50*
	MCCM–vdW	6.574	94.80	32.47	168.63	189.95
He–Ar	Reference	**6.603**	**94.16**	**32.03**	**162.10**	**175.54**
	OW	*6.577*	*91.60*	*30.74*	*158.06*	*166.89*
	MCCM–vdW	6.621	204.81	148.24	121.80	365.22
Ne–Ar	Reference	**6.604**	**205.88**	**147.97**	**124.61**	**382.24**
	OW	*6.593*	*214.04*	*154.92*	*127.94*	*402.98*
	MCCM–vdW	7.677	601.29	550.30	101.83	797.76
Kr–Kr	$a5Z+CP$	**7.691**	**606.08**	**555.18**	**103.22**	**819.63**
	OW	*7.524*	*637.16*	*584.74*	*107.04*	*881.49*

[a]"OW" refers to the values from the experimentally derived potential surface of Ogilvie and Wang (Ref. 45). The values of D_0 were calculated from the potentials with the use of Le Roy's LEVEL program (Ref. 105). The values of $\boldsymbol{\omega_e}$ and $\mathbf{k_e}$ were obtained using a harmonic approximation (see the text).

duces the reference and experimentally derived potentials quite well.

For the homodimers (Table II), the agreement of the equilibrium distances and well depths is outstanding. The largest error of R_e and D_e occurs for He–He (0.015 Bohr and 4.38 $\mu\mathrm{E}_h$, respectively). The vibrational frequencies, all of which are very small for these weakly bound systems, show errors in the range of 4.9–15.9 μa.u. For the heterodimers, the magnitude of the errors is similar. The largest error in R_e is 0.029 Bohr for He–Ar; however, this is in nearly perfect agreement with the experimentally derived potential. The largest error in D_e is only 1.75 $\mu\mathrm{E}_h$ for He–Ne.

To assess the MCCM–vdW results with regard to BSSE, an expanded version of Table II that contains values from the a5Z with and without counterpoise corrections has been included in the E-PAPS supplementary material.[85] The MCCM–vdW model provides accurate results even when the component calculations on which it is based has significant BSSE errors.

C. Application to Kr–Kr

The MCCM–vdW has been applied to the krypton dimer (Kr_2) to assess the transferability of the model to a system not present in the parameter training set. The increased number of electrons in the Kr_2 dimer prohibited use of the high-level protocol applied to the He, Ne, and Ar dimers. The highest theoretical level/basis that could be applied with available resources was CCSD(T)/a5Z without bond functions or counterpoise corrections at 20 internuclear separations. The scheme for choosing the radial points was identical to that of the He, Ne, and Ar dimers [Eq. (5)], choosing every fifth point to generate a total of 20 points (instead of 100). The experimentally derived Kr–Kr binding energy curve of Ogilvie[45] is shown in Fig. 2 along with the CCSD(T)/a5Z and MCCM–vdW binding, HF-SCF, and correlation, potential energy curves.

MCCM–vdW reproduces very well the Kr–Kr binding potential energy as calculated with CCSD(T)/a5Z. The MCCM–vdW and CCSD(T)/a5Z minimum energy distances (7.677 and 7.691 Bohr), dissociation energies (601.29 and 606.08 $\mu\mathrm{E}_h$) and vibrational force constants (797.76 and 819.63 μa.u.) agree closely. Both MCCM–vdW and CCSD(T)/a5Z agree reasonably well with the potential of Ogilvie,[45] but are slightly underbound at the minimum and along the exchange wall (see Fig. 2). The minimum energy distance of the potential of Ogilvie and Wang[45] is slightly contracted (7.524 Bohr) and the potential well is slightly deeper (637.16 $\mu\mathrm{E}_h$). The slight underbinding MCCM–vdW and CCSD(T)/a5Z at the minimum and exchange wall result in smaller vibrational force constants when compared to that of the Ogilvie and Wang potential, but agree very well with each other. The agreement between MCCM–vdW and CCSD(T)/a5Z for Kr_2 is very encouraging, not only because of the close agreement with the binding potential energy, but also of the individual HF-SCF and correlation components (Fig. 2).

For this small system, no appreciable speed-up is realized applying the MCCM–vdW relative to CCSD(T)/a5Z *without* bond functions/counterpoise corrections on an SGI Origin 2000 using MOLPRO 2000.1.[84] It should be noted that MCCM–vdW is parametrized to account implicitly for the use of bond functions and counterpoise correction.

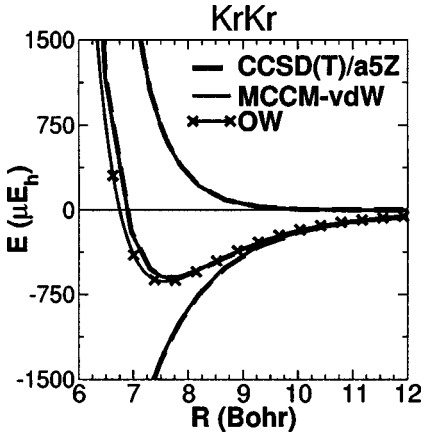

FIG. 2. A comparison of MCCM–vdW, CCSD(T)/a5Z, and experimentally derived potential energy surfaces. The experimentally derived surface "OW" is that of Ogilvie and Wang (Ref. 45).

D. Application to Rg···H_2O interactions

In this section we describe the application of the MCCM–vdW model to the interaction of rare gases with a polar molecule (water), and comparison with large basis/highly correlated calculations. The purpose here is to further validate the model with tests on systems not present in the training set, and to demonstrate transferability to systems that involve polar molecules. This is an important problem, not only from a fundamental chemical physics point of view, but also from the perspective of the design of transferable molecular simulation force fields where rare gases are often used as probes to derive nonbonded van der Waals parameters.[96–98]

To better assess the performance of the MCCM–vdW model, potential energy surfaces for rare gas–water interactions, Rg···H_2O (Rg=He, Ne, Ar), were obtained at the counterpoise-corrected CCSD(T)/a5Z level of theory with a supplementary set of $(3s3p2d)$ bond functions.[99] The set of bond functions $(3s3p3d)$ is slightly smaller than the set of bond functions used in creating the reference rare gas dimer dataset $(3s3p2d2f1g)$. There are three main reasons for using the smaller set of bond functions in this system: (1) the number of atoms in the system has doubled, making the calculation much more expensive; (2) the $(3s3p2d)$ set of bond functions was demonstrated by Tao in application to the Ar···H_2O potential energy surface to be insensitive to changes in the exponents and the placement within the bond region;[99] and (3) the Rg···H_2O data collected was not used for refinement of the MCCM–vdW parameters; rather, it was used as a validation test of the MCCM–vdW model against large basis/highly correlated calculations not present in the training set.

The details of generating the high-level Rg···H_2O data are now described. The O–H bond lengths were held fixed at 0.957 Å and the H–O–H bond angle was held fixed at 104.5°. The coordinate varied was the radial distance between the center of mass of the water and the rare gas along the C_{2v} axis of the water in the direction of the oxygen. Counterpoise-corrected binding energies at CCSD(T)/a5Z supplemented with a set of $(3s3p2d)$ bond functions[99] were obtained at 2.50, 2.75, 3.00, 3.25, 3.50, 3.75, 4.00, 4.25, 4.50, and 5.00 Å center of mass separations.

In addition to the high-level Rg···H_2O data described above, a protocol used for molecular simulation force field design (MP3/6-311++G$(3d,3p)$)[96–98] was employed for comparison. The MP3 protocol has been used to probe molecules with rare gases in order to obtain the Lennard-Jones nonbonded interaction potential parameters used in molecular mechanics calculations and molecular simulations. Table III presents the binding energy of He···H_2O, Ne···H_2O, and Ar···H_2O, as determined from MP3/6-311++G$(3d,3p)$ ($\mathbf{V}'$), MCCM–vdW ($\tilde{\mathbf{V}}$), and CCSD(T)/a5Z $(3s3p2d)$ with counterpoise correction ($\mathbf{V}$). In addition, the energy of the MCCM–vdW and reference potentials are decomposed into HF-SCF ($\tilde{\mathbf{X}}$ and $\mathbf{X}$, respectively) and correlation potential energy components ($\tilde{\mathbf{C}}$ and $\mathbf{C}$, respectively).

The agreement between the high-level and MCCM–vdW Rg···H_2O binding energies is very good. The MCCM–vdW model predicts a very slightly overbound potential for Ne···H_2O and a slightly underbound potential for He···H_2O relative to the high-level reference values. For the Ar···H_2O potential, the MCCM–vdW and high-level reference results are almost indistinguishable. The underbinding of the He···H_2O appears to be mainly due to the correlation potential, which is slightly underbound near the minimum and at larger center of mass separations. The parametrized He–He potential (Fig. 1) was also slightly underbound; hence, the observed underbinding predicted by the MCCM–vdW model for the He···H_2O system is likely related to the very weak He interactions that are notoriously difficult to capture quantum mechanically.[26,50,86–95]

The MP3/6-311++G$(3d,3p)$ protocol, which is a computationally cheaper method, does not agree as well with the high-level calculations and appears to give inconsistent results. For He···H_2O, and Ar···H_2O, MP3/6-311++G$(3d,3p)$ agrees with the high-level results beyond 4 Å, but is severely underbound near the binding potential energy minimum and along the exchange wall. On the other hand, MP3/6-311++G$(3d,3p)$ severely overbinds Ne···H_2O out to $R=5.0$ Å. At $R=3.5$ Å, MP3/6-311++G$(3d,3p)$ overbinds Ne···H_2O by a factor of 1.6 relative to the high-level data.

The close agreement between MCCM–vdW, and the reference data is encouraging, not only for the reason that neither hydrogen nor oxygen were included in the parametrization of the model, but also because electronic induction resulting from interaction with the polar water molecule plays a more prominent role. Water, which has a permanent dipole moment of around 1.85 D in the gas phase, induces a dipole on the rare gas; whereas the (practically negligible) polarization in the heteronuclear rare-gas dimer systems is caused mainly by electronegativity differences. This test is encouraging that the parametrization method adopted here may lead to more transferable quantum models.

The inclusion of attractive dispersive forces in force fields and semiempirical methods is of great importance.[100] Recently there has been an effort made to include modified pairwise core–core interactions based on *ab initio* potential

TABLE III. A comparison of MCCM–vdW, CCSD(T)/a5Z+BF+CP, and MP3/6-311++G(3*d*,3*p*) Rg···H_2O interaction energies.[a]

Rg	r (Å)	$\tilde{\mathbf{X}}$	**X**	$\tilde{\mathbf{C}}$	**C**	$\tilde{\mathbf{V}}$	**V**	**V′**
					μE_h			
Ar	2.50	26657.05	26679.56	−6709.62	−6722.48	19947.42	19957.08	21888.60
	2.75	10793.45	10806.87	−4095.57	−4135.41	6697.88	6671.46	7657.29
	3.00	4252.87	4259.25	−2560.18	−2581.62	1692.69	1677.63	2190.16
	3.25	1614.51	1615.33	−1629.90	−1632.73	−15.38	−17.40	247.54
	3.50	574.72	573.44	−1049.52	−1045.73	−474.80	−472.30	−344.23
	3.75	176.87	176.36	−680.69	−679.04	−503.82	−502.68	−449.95
	4.00	32.27	33.08	−446.14	−447.53	−413.87	−414.45	−390.90
	4.25	−14.90	−13.24	−297.20	−300.44	−312.11	−313.68	−314.93
	4.50	−26.21	−24.24	−201.80	−205.36	−228.01	−229.60	−235.81
	5.00	−21.04	−19.58	−99.80	−101.47	−120.84	−121.05	−127.29
Ne	2.50	6760.96	6738.57	−2140.52	−2023.49	4620.44	4715.08	4723.95
	2.75	2426.12	2407.77	−1308.06	−1220.23	1118.06	1187.54	1154.80
	3.00	850.11	840.38	−800.39	−750.16	49.72	90.22	−7.70
	3.25	283.37	280.15	−494.15	−468.54	−210.79	−188.39	−319.50
	3.50	83.56	84.17	−308.77	−297.05	−225.21	−212.88	−341.96
	3.75	16.70	18.33	−197.77	−191.78	−181.07	−173.45	−290.00
	4.00	−2.83	−1.96	−131.10	−126.59	−133.93	−128.55	−225.07
	4.25	−6.95	−6.87	−89.37	−84.92	−96.32	−91.79	−162.93
	4.50	−6.72	−6.96	−62.74	−58.27	−69.46	−65.23	−111.52
	5.00	−4.50	−4.55	−33.84	−29.04	−38.34	−33.59	−47.87
He	2.50	2954.39	2958.23	−971.11	−974.83	1983.28	1983.40	2248.56
	2.75	1081.51	1082.50	−577.76	−576.77	503.75	505.73	648.68
	3.00	384.14	384.36	−348.97	−348.88	35.18	35.47	118.26
	3.25	128.71	129.38	−211.74	−215.65	−83.03	−86.28	−41.30
	3.50	37.65	38.75	−129.62	−136.30	−91.97	−97.55	−78.23
	3.75	6.76	8.02	−80.59	−88.07	−73.83	−80.05	−75.31
	4.00	−2.59	−1.46	−51.31	−58.37	−53.89	−59.82	−61.69
	4.25	−4.57	−3.68	−33.95	−39.21	−38.52	−42.89	−47.38
	4.50	−4.30	−3.63	−23.69	−27.03	−27.99	−30.66	−35.10
	5.00	−2.63	−2.36	−13.38	−13.58	−16.01	−15.94	−17.96

[a]Interaction energies of MCCM–vdW, counterpoise corrected CCSD(T)/a5Z supplemented with a set of $(3s3p2d)$ bond functions, and MP3/6-311++G(3*d*,3*p*) denoted as $\tilde{\mathbf{V}}$, **V**, and **V′**, respectively. Also shown are the MCCM–vdW and CCSD(T)/a5Z+BF+CP HF-SCF and correlation components, denoted as ($\tilde{\mathbf{X}}$ and **X**) and ($\tilde{\mathbf{C}}$, **C**), respectively.

energy surfaces in order to improve the description of hydrogen bonded systems.[101,102] The creation of pairwise correlation potentials is of significant interest for the development of new semiempirical methods. One must, however, have a method for obtaining accurate correlation potentials in order to fully explore the idea. The development of the MCCM–vdW model that can reliably reproduce binding, HF-SCF and correlation energies involving rare gases is therefore of considerable interest.

The MCCM–vdW is observed to require only a fraction of the time necessary for the high-level reference data. Specifically, a MCCM–vdW single-point calculation of Ar···H_2O requires *approximately* 20% of the time necessary for the high-level reference theory as calculated on an SGI Origin 2000.

E. Application to rare-gas trimers

In this section, MCCM–vdW is applied to rare-gas trimers to demonstrate the model's ability to reproduce accurate three-body energies. Use of the MCCM–vdW model may provide a means of much more efficiently generating databases from which many-body force fields can be parametrized and/or tested. The validity of the MCCM–vdW model for the determination of three-body energies is now investigated by examining the three-body energies of Rg_3 (Rg=He, Ne, Ar).

The potential energy surface of the homonuclear trimer systems He_3, Ne_3, and Ar_3 have been studied along the radial dimension of an equilateral triangle configuration. Each angle was held fixed at 60° and the interatomic trimer distances were scaled such that they corresponded, for comparison, to the corresponding interatomic dimer distances reported by Cybulski and co-workers.[21]

The highest level calculations that could be performed on the trimer systems were at the CCSD(T)/a5Z level without bond functions or counterpoise corrections. In order to obtain the best possible binding, HF-SCF, and correlation reference potential energy curves for rare-gas clusters, the following two-body corrected model is introduced below. The analytic forms of the two-body binding, HF-SCF, and correlation reference potential energy curves at counterpoise-corrected CCSD(T)/a5Z+$(3s3p2d2f1g)$ levels for rare-gas

homo- and heterodimers involving He, Ne, and Ar have been presented and discussed in detail elsewhere.[21,83] These curves can be used to correct the two-body energy contributions for rare-gas clusters calculated with a cheaper level of theory (including the MCCM–vdW model—although the purpose here is to test the *uncorrected* MCCM–vdW model). The form of the *very high level* cluster energy model with two-body corrections, using the uncorrected theory level of CCSD(T)/a5Z, is given by

$$E^{\mathrm{VHL}} = E^{\mathrm{CCSD(T)/a5Z}} + \sum_{i<j} \Delta_{ij}, \tag{6}$$

$$E^{\mathrm{VHL}(X)} = E^{\mathrm{HF/a5Z}} + \sum_{i<j} \Delta_{ij}^{(X)}, \tag{7}$$

$$E^{\mathrm{VHL}(C)} = E^{\mathrm{VHL}} - E^{\mathrm{VHL}(X)} = E^{\mathrm{CCSD(T)/a5Z}} - E^{\mathrm{HF/a5Z}} + \sum_{i<j} \Delta_{ij}^{(C)}, \tag{8}$$

where $E^{\mathrm{CCSD(T)/a5Z}}$ and $E^{\mathrm{HF/a5Z}}$ are the energies of the rare-gas cluster at the uncorrected level of theory, and E^{VHL}, $E^{\mathrm{VHL}(X)}$, and $E^{\mathrm{VHL}(C)}$ are the corrected total, HF-SCF, and correlation energies of the clusters, respectively. The two-body correction terms are given by

$$\Delta_{ij} = E^{\mathrm{CCSD(T)/ref}}(\mathrm{Rg}_i:\mathrm{Rg}_j) - E^{\mathrm{CCSD(T)/a5Z}}(\mathrm{Rg}_i:\mathrm{Rg}_j), \tag{9}$$

$$\Delta_{ij}^{(X)} = E^{\mathrm{HF/ref}}(\mathrm{Rg}_i:\mathrm{Rg}_j) - E^{\mathrm{HF/a5Z}}(\mathrm{Rg}_i:\mathrm{Rg}_j), \tag{10}$$

$$\Delta_{ij}^{(C)} = \Delta_{ij} - \Delta_{ij}^{(X)}, \tag{11}$$

where the notation $(\mathrm{Rg}_i:\mathrm{Rg}_j)$ denotes the two-body interaction between rare-gas i and j in the cluster, obtained from a separate calculation, or in the present case, from analytic forms fitted very accurately to the two-body potential energy curves at each level of theory. These potential energy curves are available as supplementary material (E-PAPS).[85]

The reference three-body binding, HF-SCF, and correlation energies [denoted as three-body, three-body(X), and three-body(C), respectively] were calculated at the CCSD(T)/a5Z level as

$$E_{\text{3-body}}^{\mathrm{a5Z}} = E^{\mathrm{CCSD(T)/a5Z}} - \sum_{i<j} E^{\mathrm{CCSD(T)a5Z}}(\mathrm{Rg}_i:\mathrm{Rg}_j), \tag{12}$$

$$E_{\text{3-body}(X)}^{\mathrm{a5Z}} = E^{\mathrm{HF/a5Z}} - \sum_{i<j} E^{\mathrm{HF/a5Z}}(\mathrm{Rg}_i:\mathrm{Rg}_j), \tag{13}$$

$$E_{\text{3-body}(C)}^{\mathrm{a5Z}} = E_{\text{3-body}}^{\mathrm{a5Z}} - E_{\text{3-body}(X)}^{\mathrm{a5z}}. \tag{14}$$

Similarly, the MCCM–vdW three-body, three-body HF-SCF, and three-body correlation potential are defined as

$$E_{\text{3-body}}^{\mathrm{MCCM-vdW}} = E^{\mathrm{MCCM-vdW}} - \sum_{i<j} E^{\mathrm{MCCM-vdW}}(\mathrm{Rg}_i:\mathrm{Rg}_j), \tag{15}$$

$$E_{\text{3-body}(X)}^{\mathrm{MCCM-vdW}} = E^{\mathrm{MCCM-vdW}(X)} - \sum_{i<j} E^{\mathrm{MCCM-vdW}(X)}(\mathrm{Rg}_i:\mathrm{Rg}_j), \tag{16}$$

$$E_{\text{3-body}(C)}^{\mathrm{MCCM-vdW}} = E^{\mathrm{MCCM-vdW}(C)} - \sum_{i<j} E^{\mathrm{MCCM-vdW}(C)}(\mathrm{Rg}_i:\mathrm{Rg}_j), \tag{17}$$

Table IV compares the VHL reference and MCCM–vdW binding, HF-SCF, and correlation potential energy curves for the He_3, Ne_3, and Ar_3 trimer systems having C_{3v} symmetry, and Table V displays the corresponding three-body potential energy components. Overall, the MCCM–vdW model is in impressive agreement with the VHL reference curves. The MCCM–vdW HF-SCF potential, denoted MCCM–vdW(X), is slightly less repulsive than the VHL(X) potential and the correlation potential is slightly underbound for Ne_3; however, a cancellation of these small errors leads to a very accurate binding potential energy. The He_3 MCCM–vdW(C) potential energy curve is slightly underbound around the minimum of this potential energy surface relative to VHL(C) and results in a slightly underbound binding energy potential. The three-body potential energy curves from the MCCM–vdW model compare reasonably well with the CCSD(T)/a5Z data.

In general, the three-body energies (Table V) are small relative to the corresponding two-body energies. At small interatomic distances (in the repulsive region of the binding energy), the three-body energies become larger. The three-body contribution to the binding energy is generally attractive except in the region of the minimum, where it is observed to be very slightly repulsive. The three-body HF-SCF and correlation energies are attractive and repulsive, respectively. The MCCM–vdW three-body energies for Ne_3 do not agree as closely with the CCSD(T)/a5Z data as do the He_3 and Ar_3 three-body energies. The repulsive three-body correlation potential of MCCM–vdW is noticeably not repulsive enough, leading to an overall three-body potential that is nearly the same as the three-body HF-SCF potential. This is not too concerning; within the region of phase space being considered, the three-body HF-SCF energy dominates the three-body correlation energy at small distances and both become negligible at intermediate to larger distances. MCCM–vdW reproduces the CCSD(T)/a5Z three-body potentials extremely well for Ar_3 and He_3, even in the highly repulsive region of the binding potential energy.

The MCCM–vdW model is observed to be considerably accurate for rare-gas trimer systems relative to CCSD(T)/a5Z calculations. A further validation of the model is, of course, necessary, and requires the generation of highly accurate reference potential surfaces for clusters. The results reported here are nonetheless encouraging.

Although MCCM–vdW is parametrized to account for counterpoise correction with the use of bond functions, it is found to provide immense time savings for the rare-gas trimers relative to CCSD(T)/a5Z *without* the use of bond functions and without counterpoise corrections. As a specific example, a MCCM–vdW single-point calculation of Ar_3 requires *approximately* 20% of the time necessary for the

TABLE IV. A comparison of MCCM–vdW, and "Very High Level" Rg_3 trimer interaction energies.[a]

Rg	r (Å)	$\tilde{\mathbf{X}}$	X	$\tilde{\mathbf{C}}$	C	$\tilde{\mathbf{V}}$	V′
				μE_h			
Ar_3	3.000	19 003.49	18 939.28	−10 257.51	−10 025.39	8745.99	8913.88
	3.250	7903.62	7871.42	−6431.00	−6354.40	1472.62	1517.03
	3.500	3236.38	3227.17	−4076.11	−4061.27	−839.73	−834.10
	3.750	1310.55	1307.79	−2621.34	−2622.79	−1310.79	−1315.00
	3.775	1196.72	1194.15	−2510.59	−2512.35	−1313.88	−1318.20
	3.800	1092.68	1090.28	−2404.73	−2406.87	−1312.05	−1316.58
	3.850	910.72	908.61	−2208.07	−2209.94	−1297.35	−1301.33
	4.000	526.01	524.75	−1714.31	−1717.05	−1188.30	−1192.30
	4.250	207.92	208.82	−1142.21	−1143.08	−934.29	−934.26
	4.500	79.62	82.52	−776.38	−775.76	−696.76	−693.24
	5.000	8.54	12.69	−381.01	−379.95	−372.47	−367.26
	6.000	−3.53	0.34	−113.49	−112.97	−117.02	−112.63
	7.000	−1.16	0.04	−41.70	−41.80	−42.86	−41.75
Ne_3	2.250	13 336.42	13 462.18	−3329.25	−3320.54	10007.17	10 141.64
	2.500	4189.20	4290.66	−2014.41	−2081.77	2174.79	2208.89
	2.750	1277.05	1359.48	−1214.96	−1292.53	62.09	66.95
	3.000	369.70	428.55	−740.63	−799.38	−370.93	−370.84
	3.075	249.93	302.85	−641.70	−692.63	−391.77	−389.78
	3.100	218.53	269.73	−611.52	−660.21	−392.99	−390.48
	3.125	190.61	240.23	−583.05	−629.62	−392.44	−389.38
	3.250	90.97	134.56	−458.43	−497.72	−367.46	−363.17
	3.500	5.34	42.14	−286.31	−314.25	−280.97	−272.11
	3.750	−16.00	13.18	−178.57	−202.24	−194.57	−189.06
	4.000	−15.70	4.15	−110.95	−132.99	−126.65	−128.84
	4.500	−6.10	0.53	−56.14	−61.84	−62.24	−61.31
	5.000	−1.44	0.13	−30.29	−31.06	−31.73	−30.93
He_3	1.750	18 519.23	18 498.88	−3243.76	−3004.15	15 275.47	15 494.73
	2.000	6434.39	6418.84	−1733.98	−1645.31	4700.40	4773.53
	2.250	2168.39	2165.53	−940.78	−914.59	1227.61	1250.95
	2.500	712.88	713.39	−516.21	−516.21	196.66	197.18
	2.750	231.87	230.40	−287.77	−296.86	−55.90	−66.46
	2.950	94.92	92.19	−184.14	−193.86	−89.23	−101.67
	2.975	84.94	82.17	−174.46	−184.01	−89.51	−101.85
	3.000	76.02	73.22	−165.34	−174.72	−89.32	−101.50
	3.025	68.05	65.25	−156.78	−165.94	−88.73	−100.69
	3.250	24.83	23.00	−99.05	−105.67	−74.22	−82.67
	3.500	7.17	7.16	−61.87	−65.82	−54.70	−58.66
	4.000	−0.54	0.68	−26.83	−27.90	−27.37	−27.23
	5.000	−0.17	0.02	−7.08	−6.76	−7.25	−6.74

[a]The tables X, C, and V correspond to HF-SCF, correlation, and interaction (X+C) energies, respectively. The MCCM–vdW values are identified with an overtilde. The "Very High Level" values are described in the text.

high-level reference theory, as calculated on an SGI Origin 2000.

V. CONCLUSIONS

The determination of accurate *ab initio* potential energy curves for rare gases has traditionally been a challenge for quantum chemical methods. In this paper we present the development of a MCCM–vdW method for the determination of accurate potential surfaces of rare gas dimers of He, Ne, and Ar based on high-level CCSD(T) reference curves over a large range of radial points. The methods allow an accurate calculation of rare-gas dimer curves for significantly reduced computational effort and does *not* require the use of bond functions or counterpoise corrections. Consequently, this method may be used for multilevel geometry optimizations[47,82] in applications to van der Waals clusters.

Initial work in the construction of a MCCM–vdW method followed work similar to that of Fast and Truhlar.[47] However, it was found that for the design of a reliable model for dispersion interactions, several modifications were necessary. The main features of the model developed here that distinguish it from some other models include the following: (i) *the inclusion of a constraint that the coefficients sum to unity in accord with scaling arguments*; (ii) *fitting to both stationary and nonstationary points over a broad range of the two-body potential energy surface; and* (iii) *fitting simultaneously to the total binding energy and the individual Hartree–Fock and correlation energy components to produce a more transferable model*.

It has been found that the stability of the MCCM–vdW parameters increases when the model is parametrized to simultaneously reproduce binding, HF-SCF, and correlation potential energies. MCCM–vdW has been shown to be trans-

TABLE V. A comparison of MCCM–vdW and CCSD(T)/a5Z Rg_3 three-body energies.[a]

Rg	r (Å)	$\tilde{X}$	X	$\tilde{C}$	C	$\tilde{V}$	V
				μE_h			
Ar_3	3.000	−533.23	−531.00	264.23	279.68	−269.00	−251.32
	3.250	−157.87	−156.60	112.10	118.93	−45.77	−37.66
	3.500	−44.92	−44.64	47.86	47.44	2.94	2.80
	3.750	−12.37	−12.32	21.54	19.49	9.17	7.17
	3.775	−10.91	−10.82	20.26	17.91	9.36	7.09
	3.800	−9.59	−9.49	18.78	16.55	9.20	7.06
	3.850	−7.47	−7.30	15.86	14.38	8.39	7.09
	4.000	−3.76	−3.28	12.99	9.75	9.23	6.46
	4.250	−1.72	−0.81	4.31	5.83	2.59	5.02
	4.500	−1.11	−0.11	2.32	3.67	1.21	3.56
	5.000	−0.42	0.07	−0.29	1.49	−0.71	1.57
	6.000	0.16	0.07	−1.64	0.56	−1.48	0.62
	7.000	0.03	0.06	0.37	0.23	0.40	0.29
Ne_3	2.250	−261.12	−260.60	24.30	69.05	−236.83	−191.56
	2.500	−51.84	−51.86	9.45	20.33	−42.39	−31.53
	2.750	−11.51	−9.91	−0.24	5.39	−11.75	−4.52
	3.000	−3.29	−1.80	−8.65	2.06	−11.94	0.26
	3.075	−2.31	−1.06	−5.81	1.68	−8.12	0.62
	3.100	−2.06	−0.89	−7.50	1.69	−9.55	0.79
	3.125	−1.81	−0.74	−7.36	1.35	−9.17	0.62
	3.250	−0.89	−0.28	−7.20	1.11	−8.09	0.83
	3.500	0.35	0.01	−9.40	0.74	−9.04	0.75
	3.750	0.91	0.05	−6.65	0.47	−5.74	0.51
	4.000	0.84	0.07	−0.33	0.42	0.51	0.48
	4.500	0.31	0.12	−4.02	0.15	−3.71	0.27
	5.000	0.06	0.07	0.77	0.26	0.83	0.33
He_3	1.750	−1729.49	−1736.73	57.62	66.28	−1671.87	−1670.45
	2.000	−397.37	−398.43	12.80	23.17	−384.57	−375.26
	2.250	−86.52	−86.23	1.21	7.45	−85.31	−78.78
	2.500	−18.30	−17.80	−0.72	1.98	−19.02	−15.82
	2.750	−3.98	−3.60	−0.71	0.36	−4.69	−3.23
	2.950	−1.32	−1.02	−0.60	0.07	−1.92	−0.95
	2.975	−1.17	−0.88	−0.61	0.07	−1.77	−0.81
	3.000	−1.03	−0.74	−0.62	0.05	−1.65	−0.69
	3.025	−0.93	−0.62	−0.56	0.03	−1.49	−0.59
	3.250	−0.44	−0.13	−0.47	0.04	−0.91	−0.10
	3.500	−0.25	−0.01	−0.32	0.04	−0.56	0.03
	4.000	−0.02	−0.00	−0.01	0.03	−0.02	0.03
	5.000	−0.00	0.03	0.13	0.00	0.13	0.03

[a]The labels X, C, and V correspond to HF-SCF, correlation, and interation (X+C) energies, respectively. The MCCM–vdW and CCSD(T)/a5Z values are identified with and without an overtilde, respectively.

ferable to systems not contained in the training set, e.g., Kr–Kr, $Rg\cdots H_2O$ and He_3, Ne_3 and Ar_3 systems. The ability of MCCM–vdW to reproduce correlation energies may play an important role in the design and parameterization of new semiempirical methods that incorporate a treatment for long-range correlation effects. It has been shown that MCCM–vdW adequately reproduces CCSD(T)/a5Z three-body energies of rare-gas trimers, which makes the method valuable to the parametrization and testing of new many-body polarizable force fields. It is the hope that MCCM–vdW can be applied to determine potential energy surfaces of rare-gas clusters for which conventional methods of comparable accuracy are not feasible. Further testing and application to three-body and many-body potential surfaces are required before one can make solid conclusions about transferability.

Future work will involve the generation and testing of the models to more complicated potential energy surfaces. Nonetheless, this work represents an important step toward the development of more efficient quantum models to compute dispersion interactions and to obtain a systematic understanding of the transferability and many-body nature of these systems. These issues are of significant interest, not only for chemical physics, but also for the development of improved many-body molecular mechanical force fields.

ACKNOWLEDGMENTS

D.Y. is grateful for financial support provided by the National Institutes of Health (Grant No. 1R01-GM62248-01A1), and the Donors of The Petroleum Research Fund, administered by the American Chemical Society. T.G. was partially supported by a fellowship from the Chemical Physics program at the University of Minnesota and from a Na-

tional Institutes of Health Molecular Biophysics Training Grant. Computational resources were provided by the Minnesota Supercomputing Institute.

APPENDIX: THE MCCM-vdW PARAMETRIZATION PROCEDURE

The parameters in MCCM–vdW are the coefficients a_i [Eq. (1)]. These are linear parameters in the model, and can be fit using a constrained linear least-squares method. Simple scaling arguments require that the coefficients sum to unity. A singular value decomposition scheme was used to ensure the elimination of linear dependencies in the parameters.

The first step is to construct a quadratic χ^2 merit function that includes all of the homo- and heterodimer curves and is a weighted sum of squares between the high-level potential curves and the MCCM–vdW potential.

The dimer potential energy surface is denoted by a Greek index "α", $\alpha=1,...,N_\alpha$, for example $\alpha=1$, 2, 3, 4, 5, 6 corresponds to the dimers He_2, HeNe, HeAr, Ne_2, NeAr, and Ar_2, respectively (hence $N_\alpha=6$ in this work). For each dimer α, the set of radial points $r_{\alpha i}$ was defined for $i=1,...,N_p$, where the number of radial points $N_p=100$ here. Similarly, the level of theory/basis set is denoted by the index "j", $j=1,...,N_T$, where N_T is the number of theory/basis set combinations.[103]

Let $v_\alpha(r_{\alpha i})$ denote the elements of an $(N_\alpha \cdot N_p)\times 1$ column vector $\mathbf{v}$ containing the values of the high-level reference binding energy for the dimer α at the radial point $r_{\alpha i}$. Similarly, let $x_\alpha(r_{\alpha i})$ and $c_\alpha(r_{\alpha i})$ denote the elements of $(N_\alpha \cdot N_p)\times 1$ column vectors $\mathbf{x}$ and $\mathbf{c}$ containing the values of the high-level reference HF-SCF and correlation energies, respectively. In the literature, the repulsive part of the rare-gas interaction is sometimes referred to as an "exchange" term (motivating the "$\mathbf{x}$" label); however, this terminology is avoided so as not to be confused with Hartree–Fock exchange energy that has a different meaning in quantum chemistry.

Here a supermatrix notation has been introduced where the indexes α and i are treated together as a single combined index "αi." The model potentials $\tilde{v}_\alpha(r_{\alpha i})$, $\tilde{x}_\alpha(r_{\alpha i})$, and $\tilde{c}_\alpha(r_{\alpha i})$ are constructed as a linear combination of N_T theory/basis set levels:

$$\tilde{v}_\alpha(r_{\alpha i})=\sum_{j=1}^{N_T} V_\alpha(r_{\alpha i})_j \cdot a_j, \tag{A1}$$

$$\tilde{x}_\alpha(r_{\alpha i})=\sum_{j=1}^{N_T} X_\alpha(r_{\alpha i})_j \cdot a_j, \tag{A2}$$

$$\tilde{c}_\alpha(r_{\alpha i})=\sum_{j=1}^{N_T} C_\alpha(r_{\alpha i})_j \cdot a_j, \tag{A3}$$

where $V_\alpha(r_{\alpha i})_j$ is the binding energy of the αth dimer at the ith radial point $(r_{\alpha i})$ and jth theory/basis set level, and a_j is the coefficient in the MCCM–vdW for that level. Similarly, $X_\alpha(r_{\alpha i})_j$ and $C_\alpha(r_{\alpha i})_j$ are the corresponding HF-SCF and correlation potential energies, respectively, at the same radial point $(r_{\alpha i})$ and theory/basis set level. Note: there is only *one* set of parameters $\{a_j\}$ used for all three MCCM–vdW model potential energy components, and that the correlation energy is defined to be zero for all HF theory levels. Using a supermatrix formulation, these equations can be written concisely as

$$\tilde{\mathbf{v}}=\mathbf{V}\cdot\mathbf{a}, \tag{A4}$$

$$\tilde{\mathbf{x}}=\mathbf{X}\cdot\mathbf{a}, \tag{A5}$$

$$\tilde{\mathbf{c}}=\mathbf{C}\cdot\mathbf{a}, \tag{A6}$$

where $\tilde{v}_{\alpha i}\equiv\tilde{v}_\alpha(r_{\alpha i})$, $\tilde{x}_{\alpha i}\equiv\tilde{x}_\alpha(r_{\alpha i})$, $\tilde{c}_{\alpha i}\equiv\tilde{c}_\alpha(r_{\alpha i})$, $V_{\alpha i,j}\equiv V_\alpha(r_{\alpha i})_j$, $X_{\alpha i,j}\equiv X_\alpha(r_{\alpha i})_j$, and $C_{\alpha i,j}\equiv C_\alpha(r_{\alpha i})_j$.

Consider the merit function χ^2,

$$\chi^2(\mathbf{a};\omega_v,\omega_x,\omega_c,S)=\omega_v\chi_v^2(\mathbf{a};S)+\omega_x\chi_x^2(\mathbf{a};S)+\omega_c\chi_c^2(\mathbf{a};S), \tag{A7}$$

where S indicates the training set of molecules used to construct the merit function, and ω_v, ω_x, and ω_c are empirical parameters that scale the individual χ^2 functions for the binding, HF-SCF, and correlation potential energies, defined by

$$\chi_v^2(\mathbf{a};S)=\frac{1}{2}\sum_\alpha^S\sum_i w_{\alpha i}(\tilde{v}_{\alpha i}-v_{\alpha i})^2=\frac{1}{2}(\tilde{\mathbf{v}}-\mathbf{v})^T\cdot\mathbf{W}\cdot(\tilde{\mathbf{v}}-\mathbf{v}), \tag{A8}$$

$$\chi_x^2(\mathbf{a};S)=\frac{1}{2}\sum_\alpha^S\sum_i w_{\alpha i}(\tilde{x}_{\alpha i}-x_{\alpha i})^2=\frac{1}{2}(\tilde{\mathbf{x}}-\mathbf{x})^T\cdot\mathbf{W}\cdot(\tilde{\mathbf{x}}-\mathbf{x}), \tag{A9}$$

$$\chi_c^2(\mathbf{a};S)=\frac{1}{2}\sum_\alpha^S\sum_i w_{\alpha i}(\tilde{c}_{\alpha i}-c_{\alpha i})^2=\frac{1}{2}(\tilde{\mathbf{c}}-\mathbf{c})^T\cdot\mathbf{W}\cdot(\tilde{\mathbf{c}}-\mathbf{c}). \tag{A10}$$

Here the summation over α runs over the molecules included in the training set S, $w_{\alpha i}$ is the weight for the α dimer curve at the radial point $r_{\alpha i}$, and $\mathbf{W}$ is the corresponding $(N_\alpha \cdot N_p)\times(N_\alpha \cdot N_p)$ diagonal weight matrix defined by $W_{\alpha i,\alpha' i'}=w_{\alpha i}\cdot\delta_{\alpha i,\alpha' i'}$. Equation (A7) can be rewritten as

$$\chi^2(\mathbf{a};\omega_v,\omega_x,\omega_c,S)=\tfrac{1}{2}\mathbf{a}^T\cdot\mathbf{B}\cdot\mathbf{a}-\mathbf{a}^T\cdot\mathbf{g}+\text{const}, \tag{A11}$$

where

$$\mathbf{B}=\omega_v\mathbf{V}^T\cdot\mathbf{W}\cdot\mathbf{V}+\omega_x\mathbf{X}^T\cdot\mathbf{W}\cdot\mathbf{X}+\omega_c\mathbf{C}^T\cdot\mathbf{W}\cdot\mathbf{C}, \tag{A12}$$

$$\mathbf{g}=\omega_v\mathbf{V}^T\cdot\mathbf{W}\cdot\mathbf{v}+\omega_x\mathbf{X}^T\cdot\mathbf{W}\cdot\mathbf{x}+\omega_c\mathbf{C}^T\cdot\mathbf{W}\cdot\mathbf{c}, \tag{A13}$$

$$\text{const}=\omega_v\mathbf{v}^T\cdot\mathbf{W}\cdot\mathbf{v}+\omega_x\mathbf{x}^T\cdot\mathbf{W}\cdot\mathbf{x}+\omega_c\mathbf{c}^T\cdot\mathbf{W}\cdot\mathbf{c}. \tag{A14}$$

The vector of fit parameters $\mathbf{a}$ are obtained from the constrained variational condition

$$\delta\{\chi^2(\mathbf{a};\omega_v,\omega_x,\omega_c,S)-\lambda(\mathbf{a}^T\cdot\mathbf{1}-1)\}=0, \tag{A15}$$

where $\mathbf{1}$ is an $N_T\times 1$ column vector with each element equal to 1. The solution of Eq. (A15) leads to

$$\mathbf{a}=\mathbf{B}^{-1}\cdot(\mathbf{g}+\lambda\mathbf{1}), \tag{A16}$$

where the Lagrange multiplier λ is chosen to satisfy the constraint condition $\mathbf{a}^T \cdot \mathbf{1} = 1$,

$$\lambda = (1 - \mathbf{1}^T \cdot \mathbf{g})/(\mathbf{1}^T \cdot \mathbf{B}^{-1} \cdot \mathbf{1}). \quad \text{(A17)}$$

The matrix inverse in Eqs. (A16) and (A17) were performed using singular value decompositions[104] using a threshold of 10^{-8} for the singular values.

The choice of the radial weights $w_{\alpha i}$ (and hence the diagonal weight matrix $\mathbf{W}$) was key to obtaining accurate results in the physically most relevant regions of the potential energy curves. Many forms of the weight function were explored, and the one that was found to provide the best balance of simplicity and overall reliability was of the form

$$w_{\alpha i} = \frac{g_{\alpha i}}{\Sigma_{\alpha' i'} g_{\alpha' i'}}, \quad \text{(A18)}$$

where

$$g_{\alpha i} = \exp[-\beta \cdot v_\alpha^0(r_{\alpha i})/D_e(\alpha)]\Delta r_{\alpha i}, \quad \text{(A19)}$$

where the parameter $\beta = 0.5$, $D_e(\alpha)$ is the energy minimum of the reference potential binding curve, and $\Delta r_{\alpha i}$ is the finite difference radial distance between adjacent radial points; i.e., $\Delta r_{\alpha i} = r_{\alpha(i+1)} - r_{\alpha(i-1)}$. The purpose of the $\Delta r_{\alpha i}$ is to take into account the nonuniform distribution of radial sample points given in Eq. (5).

The weights ω_v, ω_x, and ω_c were also instrumental in deriving a transferable model, as discussed in greater detail in the following section. As a specific example, if in Eq. (A7) the parameters were set to $\omega_v = 1$ and $\omega_x = \omega_c = 0$, then the chi-squared function $\chi^2(\mathbf{a};1,0,0,S)$ would consider only the total binding potential energy of the dataset S in the fitting procedure. After considerable testing, values of $\omega_v = 0.8$, $\omega_x = 0.1$, and $\omega_c = 0.1$ were chosen for the present work. A further discussion of these parameters is presented in Sec. IV A.

[1] G. Chałasiński and M. Gutowski, Chem. Rev. (Washington, D.C.) **88**, 943 (1988).
[2] G. Chałasiński and M. M. Szczęśniak, Chem. Rev. (Washington, D.C.) **94**, 1723 (1994).
[3] G. Chałasiński and M. M. Szczęśniak, Chem. Rev. (Washington, D.C.) **100**, 4227 (2000).
[4] C. E. H. Dessent and K. Müller-Dethlefs, Chem. Rev. (Washington, D.C.) **100**, 3999 (2000).
[5] K. R. Leopold, G. T. Fraser, S. E. Novick, and W. Klemperer, Chem. Rev. (Washington, D.C.) **94**, 1807 (1994).
[6] R. Burcl, P. Piecuch, V. Špirko, and O. Bludsky, Int. J. Quantum Chem. **80**, 916 (2000).
[7] S. Hirata, M. N. I. Grabowski, and R. J. Bartlett, J. Chem. Phys. **114**, 3919 (2001).
[8] P. Jungwirth and A. I. Krylov, J. Chem. Phys. **115**, 10214 (2001).
[9] S. A. Kucharski, M. Kolaski, and R. J. Bartlett, J. Chem. Phys. **114**, 692 (2001).
[10] M. Nooijen, Phys. Rev. Lett. **84**, 2108 (2000).
[11] M. Nooijen and R. J. Bartlett, Int. J. Quantum Chem. **63**, 601 (1997).
[12] T. van Voorhis and M. Head-Gordon, J. Chem. Phys. **115**, 7814 (2001).
[13] T. van Voorhis and M. Head-Gordon, J. Chem. Phys. **115**, 5033 (2001).
[14] H. Koch, O. Christiansen, P. Jørgensen, A. Sanchez de Merás, and T. Helgaker, J. Chem. Phys. **106**, 1808 (1997).
[15] T. van Mourik and R. J. Gdanitz, J. Chem. Phys. **116**, 9620 (2002).
[16] J. F. Dobson and J. Wang, Phys. Rev. Lett. **82**, 2123 (1999).
[17] M. Lein, J. F. Dobson, and E. K. Gross, J. Comput. Chem. **20**, 12 (1999).
[18] J. M. Pérez-Jordá, E. San-Fabián, and A. J. Pérez-Jiménez, J. Chem. Phys. **110**, 1916 (1999).
[19] Y. Zhang, W. Pan, and W. Yang, J. Chem. Phys. **107**, 7921 (1997).
[20] E. Engle and A. F. Bonetti, Int. J. Mod. Phys. B **15**, 1703 (2001).
[21] S. M. Cybulski and R. R. Toczylowski, J. Chem. Phys. **111**, 10520 (1999).
[22] B. Fernández, C. Hättig, H. Koch, and A. Rizzo, J. Chem. Phys. **110**, 2872 (1999).
[23] B. Fernández and H. Koch, J. Chem. Phys. **109**, 10255 (1998).
[24] H. Koch, B. Fernández, and O. Christiansen, J. Chem. Phys. **108**, 2784 (1998).
[25] H. Koch, C. Hättig, H. Larsen, J. Olsen, P. J. Rgensen, B. Fernández, and A. Rizzo, J. Chem. Phys. **111**, 10108 (1999).
[26] T. van Mourik and T. H. Dunning, Jr., J. Chem. Phys. **111**, 9248 (1999).
[27] T. van Mourik and J. H. van Lenthe, J. Chem. Phys. **102**, 7479 (1995).
[28] T. van Mourik, A. K. Wilson, and T. H. Dunning, Jr., Mol. Phys. **96**, 529 (1999).
[29] T. H. Dunning, Jr., J. Chem. Phys. **90**, 1007 (1989).
[30] T. H. Dunning, Jr., K. A. Peterson, and A. K. Wilson, J. Chem. Phys. **114**, 9244 (2001).
[31] T. H. Dunning, Jr. and K. A. Peterson, J. Chem. Phys. **113**, 7799 (2000).
[32] R. A. Kendall, T. H. Dunning, Jr., and R. J. Harrison, J. Chem. Phys. **96**, 6796 (1992).
[33] T. van Mourik and T. H. Dunning, Jr., Int. J. Quantum Chem. **76**, 205 (2000).
[34] A. K. Wilson, T. van Mourik, and T. H. Dunning, Jr., J. Mol. Struct. **388**, 339 (1996).
[35] D. E. Woon and T. H. Dunning, Jr., J. Chem. Phys. **98**, 1358 (1993).
[36] D. E. Woon and T. H. Dunning, Jr., J. Chem. Phys. **100**, 2975 (1994).
[37] D. E. Woon and T. H. Dunning, Jr., J. Chem. Phys. **103**, 4572 (1995).
[38] H. Partridge and C. W. Bauschlicher, Jr., Mol. Phys. **96**, 705 (1999).
[39] F.-M. Tao, J. Chem. Phys. **98**, 2481 (1993).
[40] F.-M. Tao, J. Chem. Phys. **98**, 3049 (1993).
[41] F.-M. Tao, J. Chem. Phys. **100**, 4947 (1994).
[42] F. Tao, Int. Rev. Phys. Chem. **20**, 617 (2001).
[43] F.-M. Tao and Y.-K. Pan, J. Chem. Phys. **97**, 4989 (1992).
[44] T. J. Giese, V. M. Audette, and D. M. York, J. Chem. Phys. (in press).
[45] J. F. Ogilvie and F. Y. Wang, J. Mol. Struct. **273**, 277 (1992).
[46] J. Ogilvie and F. Y. Wang, J. Mol. Struct. **291**, 313 (1993).
[47] P. Fast, D. Truhlar, J. Phys. Chem. A **103**, 5129 (1999).
[48] L. A. Curtiss, C. Jones, G. W. Trucks, K. Raghavachari, and J. A. Pople, J. Chem. Phys. **93**, 2537 (1990).
[49] J. A. Pople, M. Head-Gordon, D. J. Fox, K. Raghavachari, and L. A. Curtiss, J. Chem. Phys. **90**, 5622 (1989).
[50] R. A. Aziz and M. J. Slaman, J. Chem. Phys. **94**, 8047 (1991).
[51] R. A. Aziz and M. J. Salman, Mol. Phys. **58**, 679 (1986).
[52] R. A. Aziz and M. J. Slaman, Mol. Phys. **57**, 825 (1965).
[53] R. A. Aziz and M. J. Slaman, Chem. Phys. **130**, 187 (1989).
[54] R. A. Aziz, W. J. Meath, and A. R. Allnatt, Chem. Phys. **78**, 295 (1983).
[55] D. A. Barrow, M. J. Slaman, and R. A. Aziz, J. Chem. Phys. **91**, 6348 (1989).
[56] R. A. Aziz and A. van Dalon, J. Chem. Phys. **78**, 2413 (1983).
[57] R. A. Aziz, A. van Dalen, J. Chem. Phys. **78**, 2402 (1983).
[58] D. A. Barrow, M. J. Slaman, and R. A. Aziz, J. Chem. Phys. **96**, 5555 (1992).
[59] Y.-P. Liu, K. Kim, B. J. Berne, R. A. Friesner, and S. W. Rick, J. Chem. Phys. **108**, 4739 (1998).
[60] N. Foloppe and A. D. MacKerell, Jr., J. Comput. Chem. **21**, 86 (2000).
[61] T. A. Halgren and W. Damm, Curr. Opin. Struct. Biol. **11**, 236 (2001).
[62] S. F. Boys and F. Bernardi, Mol. Phys. **19**, 553 (1970).
[63] F. B. van Duijneveldt, J. van Duijneveldt-van de Rijdt, and J. H. van Lenthe, Chem. Rev. (Washington, D.C.) **94**, 1873 (1994).
[64] T. H. Dunning, Jr., J. Phys. Chem. A **104**, 9062 (2000).
[65] Y. Chuang and D. G. Truhlar, J. Phys. Chem. A **103**, 651 (1999).
[66] L. A. Curtiss, J. E. Carpenter, K. Raghavachari, and J. A. Pople, J. Chem. Phys. **96**, 9030 (1992).
[67] L. A. Curtiss, K. Raghavachari, and J. A. Pople, J. Chem. Phys. **103**, 4192 (1995).
[68] L. A. Curtiss, K. Raghavachari, P. C. Redfern, and J. A. Pople, J. Chem. Phys. **106**, 1063 (1997).
[69] L. A. Curtiss, K. Raghavachari, P. C. Redfern, and J. A. Pople, J. Chem. Phys. **112**, 7374 (2000).
[70] L. A. Curtiss, K. Raghavachari, P. C. Redfern, and J. A. Pople, J. Chem. Phys. **112**, 1125 (2000).
[71] L. A. Curtiss, K. Raghavachari, P. C. Redfern, V. Rassolov, and J. A. Pople, J. Chem. Phys. **109**, 7764 (1998).
[72] L. A. Curtiss, P. C. Redfern, K. Raghavachari, and J. A. Pople, Chem. Phys. Lett. **313**, 600 (1999).

[73] L. A. Curtiss, P. C. Redfern, K. Raghavachari, and J. A. Pople, J. Chem. Phys. **114**, 108 (2001).
[74] L. A. Curtiss, P. C. Redfern, K. Raghavachari, V. Rassolov, and J. A. Pople, J. Chem. Phys. **110**, 4703 (1999).
[75] L. A. Curtiss, P. C. Redfern, V. Rassolov, G. Kedziora, and J. A. Pople, J. Chem. Phys. **114**, 9287 (2001).
[76] P. L. Fast, J. Corchado, M. L. Sanchez, and D. G. Truhlar, J. Phys. Chem. A **103**, 3139 (1999).
[77] P. L. Fast, M. Luz Sánchez, and D. G. Truhlar, Chem. Phys. Lett. **306**, 407 (1999).
[78] P. L. Fast, N. E. Schultz, and D. G. Truhlar, J. Phys. Chem. A **105**, 4143 (2001).
[79] P. L. Fast and D. G. Truhlar, J. Phys. Chem. A **104**, 6111 (2000).
[80] J. M. Rodgers, P. L. Fast, D. G. Truhlar, J. Chem. Phys. **112**, 3141 (2000).
[81] T. N. Truong, D. G. Truhlar, K. K. Baldridge, M. S. Gordon, and R. Steckler, J. Chem. Phys. **90**, 7137 (1989).
[82] J. M. Rodgers, B. J. Lynch, P. L. Fast, Y.-Y. Chuang, and D. G. Truhlar, MULTILEVEL version 1.0, University of Minnesota, 1999 (http://comp.chem.umn.edu/multilevel).
[83] T. J. Giese, V. M. Audette, and D. M. York, J. Chem. Phys. **119**, 2618 (2003).
[84] MOLPRO is a package of *ab initio* programs written by H.-J. Werner and P. J. Knowles, with contributions from R. D. Amos, A. Bernhardsson, A. Berning *et al.*
[85] See EPAPS Document No. E-JCPSA6-120-304402 for further discussion. A direct link to this document may be found in the online article's HTML reference section. The document may also be reached via the EPAPS homepage (http://www.aip.org/pubservs/epaps.html) or from ftp.aip.org in the directory /epaps/. See the EPAPS homepage for more information.
[86] J. B. Anderson, C. A. Traynor, and B. M. Boghosian, J. Chem. Phys. **99**, 345 (1993).
[87] A. R. Janzen and R. A. Aziz, J. Chem. Phys. **107**, 914 (1997).
[88] R. Bukowski, B. Jeziorski, and K. Szalewicz, J. Chem. Phys. **104**, 3306 (1996).
[89] R. J. Gdanitz, J. Chem. Phys. **113**, 5145 (2000).
[90] W. Klopper and J. Noga, J. Chem. Phys. **103**, 6127 (1995).
[91] W. Klopper, J. Chem. Phys. **115**, 761 (2001).
[92] T. Korona, H. L. Williams, R. Bukowski, B. Jeziorski, and K. Szalewicz, J. Chem. Phys. **106**, 5109 (1997).
[93] K. T. Tang, J. P. Toennies, and C. L. Yiu, Phys. Rev. Lett. **74**, 1546 (1995).
[94] K. T. Tang and J. P. Toennies, J. Chem. Phys. **118**, 4976 (2003).
[95] M. Jeziorska, R. Bukowski, W. Cencek, M. Jaszunski, B. Jeziorski, and K. Szalewicz, Collect. Czech. Chem. Commun. **68**, 463 (2003).
[96] D. Yin and A. D. MacKerell, Jr., J. Phys. Chem. **100**, 2588 (1996).
[97] D. Yin and A. D. MacKerell, Jr., J. Comput. Chem. **19**, 334 (1998).
[98] C. I. Jen and A. D. M. Daxu Yin, J. Comput. Chem. **23**, 199 (2002).
[99] F. Tao and W. Klemperer, J. Chem. Phys. **101**, 1129 (1994).
[100] W. Thiel, in *Advances in Chemical Physics*, edited by I. Prigogine and S. A. Rice (Wiley, New York, 1996), Vol. 93, pp. 703–757.
[101] M. Bernal-Uruchurtu and M. Ruiz-López, Chem. Phys. Lett. **330**, 118 (2000).
[102] M. I. Bernal-Uruchurtu, M. T. C. Martins-Costa, and C. Millot, and M. F. Ruiz-Lòpez, J. Comput. Chem. **21**, 572 (2000).
[103] There are a total of 16 possible levels of theory/basis set combinations, only ten of which were used in this work. The particular combinations used are given in the tables and in Eq. (1).
[104] W. H. Press, S. A. Teukolsky, W. T. Vetterling, and W. P. Flannery, *Numerical Recipes in FORTRAN*, 2nd ed. (Cambridge University Press, Cambridge, 1992).
[105] R. J. Le Roy, LEVEL 7.5: A Computer Program for Solving the Radial Schrödinger Equation for Bound and Quasibound Levels, University of Waterloo Chemical Physics Research Report CP-655 (2002). The source code and manual for this program may be obtained from the ''Computer Programs'' link on the www site http://leroy.waterloo.ca